Applied Mechanics and Materials
ISSN: 1662-7482, Vol. 876, pp 52-56
doi:10.4028/www.scientific.net/AMM.876.52

Submitted: 2017-06-25
Revised: 2017-08-07
Accepted: 2017-09-06
Online: 2018-02-01

High Photocatalytic Activity of Oliver-Like $BiVO_4$ for Rhodamine B Degradation under Visible Light Irradiation

Huu Vinh Nguyen[1,a], Tran Van Thuan[1,b], Sy Trung Do[2,c], Duy Trinh Nguyen[1,d], Dai-Viet N. Vo[3,e] and Long Giang Bach[1,f*]

[1]NTT Institute of Hi-Technology, Nguyen Tat Thanh University, Ho Chi Minh City, Vietnam

[2]Laboratory of Material and Environment Technology, Institute of Chemistry, VAST, Hanoi, Vietnam

[3]Faculty of Chemical & Natural Resources Engineering, Universiti Malaysia Pahang, Malaysia

[a]nhvinh@ntt.edu.vn, [b]tvthuan@ntt.edu.vn, [c]dosyvhh@gmail.com, [d]ndtrinh@ntt.edu.vn, [e]vietvo@ump.edu.my, [f*]blgiang@ntt.edu.vn

Keywords: $BiVO_4$ crystals, Solvent-driven synthesis, Photocatalytic activity, Visible light irradiation.

Abstract. We report the facial synthesis of $BiVO_4$ crystals with different morphologies by the solvothermal and hydrothermal process. The phase structure and morphology as-synthesized samples were characterized by XRD, FE-SEM, and UV-vis DRS spectroscopy. We also investigated the photocatalytic activity of $BiVO_4$ for the decomposition of rhodamine B (RhB) under visible light irradiation. The results showed that oliver-like $BiVO_4$ was obtained when using the mixed solvent of ethylene glycol and water while starflower-like $BiVO_4$ was obtained using the mixed solvent of ethylene glycol monomethyl ether and water. The hydrothermal evolution process the $BiVO_4$ product with a rod-like morphology. Oliver-like $BiVO_4$ with pure monoclinic scheelite phase and high specific surface area exhibits efficient photodegradation of RhB ($k = 7.82x10^{-3}$ min^{-1}).

Introduction

Bismuth (III) vanadate ($BiVO_4$) has been paid much attention in photocatalytic applications. It exhibits high photooxidative capabilities for O_2 evolution from water, carbon dioxide reduction, and organic pollutants decomposition under visible-light irradiation [1–3]. $BiVO_4$ crystal exists in three crystal structure types: monoclinic scheelite (s-m $BiVO_4$), tetragonal zircon (z-t $BiVO_4$) and tetragonal scheelite (s-t $BiVO_4$) structure [4]. Among them, s-m $BiVO_4$ shows the highest visible-light-driven photocatalyst because it possesses a narrow ban gap (2.4 eV). However, the poor charge-transport characteristics and the weak surface adsorption properties lead to excessive electro-hole recombination, which limits its overall photocatalytic efficiency.

Many methods have been utilized to prepare $BiVO_4$, such as sol –gel methods, co-precipitation, hydrothermal, and solvothermal method [5–8]. However, the effect of the solvent on the morphology and photocatalytic activity of $BiVO_4$ has not been reported carefully. Herein, we synthesized $BiVO_4$ by both methods: solvothermal and hydrothermal method. Ethylene glycol (EG), ethylene glycol monomethyl ether (EM) and H_2O act as solvents with different polarities. Their activity as-photocatalysts for the decomposition of rhodamine B (RhB) was also investigated.

Materials and Methods

In a typical synthesis, $Bi(NO_3)_3$ (4 mmol) and an equal amount of NH_4VO_3 were dissolved into 70 mL EG and 10 mL water, respectively. Then, these two solutions were mixed together and adjusted pH ≈ 7 by NH_3 and HNO_3 solution. The mixed solution was continuously stirred for 1 h before being transferred into a 100 mL Teflon-lined stainless steel autoclave and heated at 100 ^oC for 12 h. The obtained suspension was centrifuged at 6000 rpm for 30 minutes, and the yellow solids were rinsed with water for five times, dried at 110 ^oC for 12 h. The sample synthesized in EG was noted BV-EG. For comparison, the other sample was synthesized in EM (noted BV-EM) by replacing EG with EM while keeping other parameters the same. Another sample was also prepared using only H_2O as a solvent, denoted as BV-H_2O.

The crystal phase was examined by powder X-ray diffraction (XRD) patterns with Cu Kα radiation (D8 Advance Bruker powder diffractometer, Germany). Surface morphologies of the products were observed by scanning electron microscopy (SEM, JSM-5300 LV, Jeol, Japan). The optical properties of the products were recorded on a Shimadzu UV-vis spectrophotometer. Specific surface areas of the samples were measured by BET method (N_2 adsorption) with Micromeritics 2020 volumetric adsorption analyzer system.

Photocatalytic activities of the samples were calculated by the decomposition of RhB under visible region with a 300W Xe-arc lamp (Oriel) and a 420 nm cut-off filter. The reactor was filled with a mixture of RhB aqueous solution (10^{-5} M, 100 mL) and the given photocatalyst (100 mg). Before lighting on, the solution was magnetically stirred in the dark for 60 minutes to establish adsorption-desorption equilibrium. At given time intervals, 5 mL of the suspension was withdrawn and then centrifuged for absorbance analysis by UV–Vis spectrometer at 554 nm.

Results and Discussion

XRD patterns of the as-synthesized $BiVO_4$ samples in different solvents are shown in Fig. 1. When $BiVO_4$ synthesized by using EG, all of the diffraction peaks could be indexed as the single phase s-m $BiVO_4$ (JCPDS 14-0688) with the presence of peaks $2\theta = 29^o$ and the splitting of peaks at 18.5^o, 35^o and 46^o, corresponding to the patterns reported earlier [4,9]. The monoclinic phase $BiVO_4$ was also synthesized in the present of EM because the XRD pattern depicted that the main phase was similar to that of m-s $BiVO_4$. However, XRD pattern of the product also exhibited the existence of z-t $BiVO_4$ (JCPDS 14-00133) with the present of peak $2\theta = 24.4^o$ and 32.9^o. The $BiVO_4$ sample was also synthesized by a hydrothermal method, XRD pattern of the product exhibited a pattern similar to that of z-t $BiVO_4$ with the coexistence of Bi_2O_3 resulting from hydrolysis of $Bi(NO_3)_3$. As shown in earlier reports, EG and EM can coordinate with Bi^{3+} to form EG or EM-Bi complexes [10–14]. EG or EM-Bi complexes with strong chelating ability can hinder the water molecules approaching to Bi^{3+}, and therefore, s-m $BiVO_4$ crystals can be favorably formed. In the water media, the water molecules easily approach to Bi^{3+}, which led to the formation of z-t phase. In the present of EM, EM can provide a weaker caging effect and the complexes due to EM can be broken under solvothermal treatment, resulting the water molecules can still approach to Bi^{3+} to produce z-t phase.

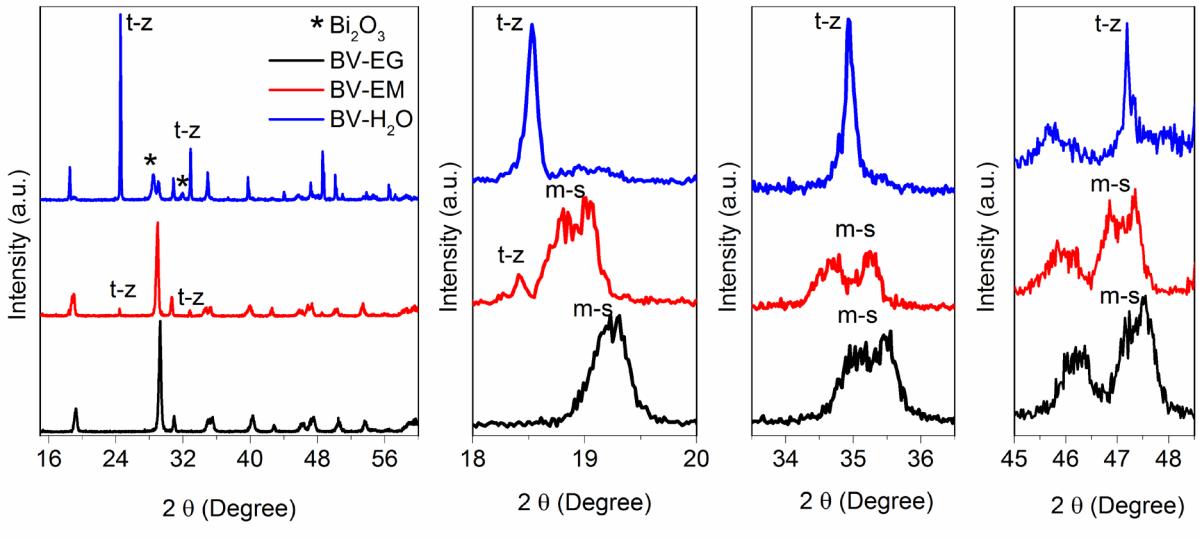

Fig. 1 XRD patterns of $BiVO_4$ samples.

Fig. 2 showed FE-SEM images of the as-prepared $BiVO_4$ samples synthesized in different solvents. It can be seen the effect of solvent on surface morphologies and particle shapes of the $BiVO_4$ samples. $BiVO_4$ synthesized by using EG as a solvent exhibited olive-like morphologies with the coexistence of small irregular particles, as shown in Fig. 2(a). Starflower-like $BiVO_4$ was obtained when EM was used as the solvent (Fig. 2(b)). The $BiVO_4$ product with a rod-like morphology was also obtained when only H_2O was used as the solvent (Fig. 2(c)). It is said that the polarity and

viscosity of the solvents have a remarkable influence on the morphologies of $BiVO_4$. As mentioned above, EM and EG can coordinate with Bi^{3+} to form EM or EG-Bi complexes and then react with VO_4^{3-} to form the primary $BiVO_4$ colloidal nanoparticles. The primary $BiVO_4$ colloidal nanoparticles in EG media gathered into oriented 3D aggregates by the assembly to minimize their surface area and to decrease their energy in the solvothermal process. When H_2O use as a solvent with low viscosity favored the growth of 1D nanorod [1].

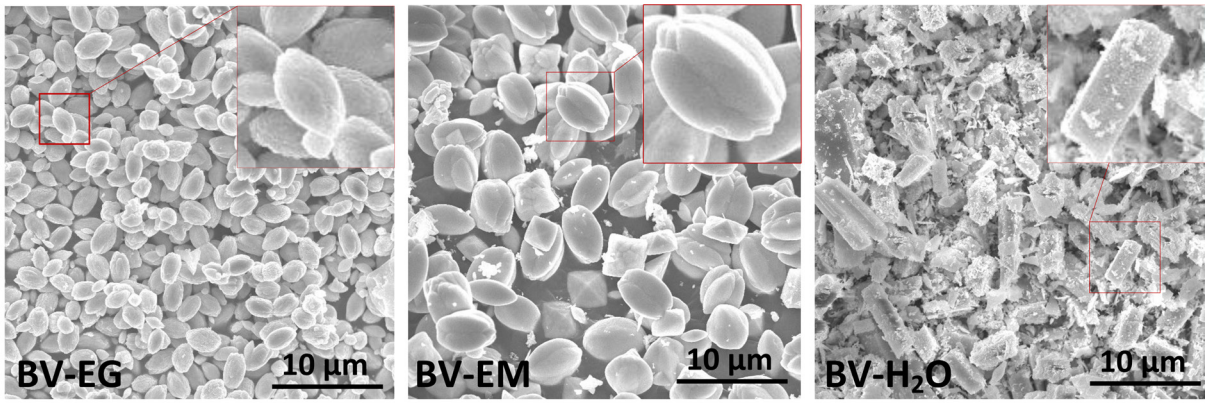

Fig. 2 SEM images of $BiVO_4$ samples.

UV-Vis DRS spectra of the as-obtained $BiVO_4$ products are shown in Fig. 3(a). As shown in Fig. 3(a), compared to TiO_2-P25, all the catalysts displayed strong absorption in visible light range, and thus the photocatalytic property of $BiVO_4$ materials was enhanced in the visible region. The indirect band gap energy (Eg) of all samples were calculated from the tangent line in the plots of the modified Kubelka–Munk function $[F(R'_\infty)h\theta]^{1/2}$ versus photon energy. The band gap values of the various samples are reported in Table 1.

Table 1. The physical properties and photocatalytic activity of TiO_2-P25 and $BiVO_4$ samples.

Sample	**S_{BET} (m^2/g)**	**E_g (eV)**	**k ($x10^{-3}min^{-1}$)**
TiO_2-P25	-	3.15	0.71
BV-EG	105	2.31	7.82
BV-EM	73	2.29	4.05
BV-H_2O	72	2.44	4.43

Fig. 3(b) displays the decomposition rates of RhB over $BiVO_4$ samples. The sample prepared in EG shows the highest photocatalytic activity in the photodegradation of RhB under visible light irradiation. The photodecomposition rate constant (k) of RhB over photocatalysts, as estimated from a pseudo-first order reaction kinetic model: $\ln(C_o/C) = kt$, were summarized in Table 1. The k value of $BiVO_4$ sample prepared in EG was $7.82x10^{-3}$ min^{-1}, is higher than that of s-m $BiVO_4$ prepared in EM and s-t $BiVO_4$ prepared in H_2O. The enhanced photocatalytic activity of $BiVO_4$ samples is most probably related to the morphology and structure phase of $BiVO_4$ [4]. Previous reports demonstrated that only pure s-m $BiVO_4$ shows the highest visible-light-driven photocatalyst in three structure phase of $BiVO_4$. Besides, a 3D ellipsoidal sphere with uniform and small size exhibited the better photocatalytic activity [16].

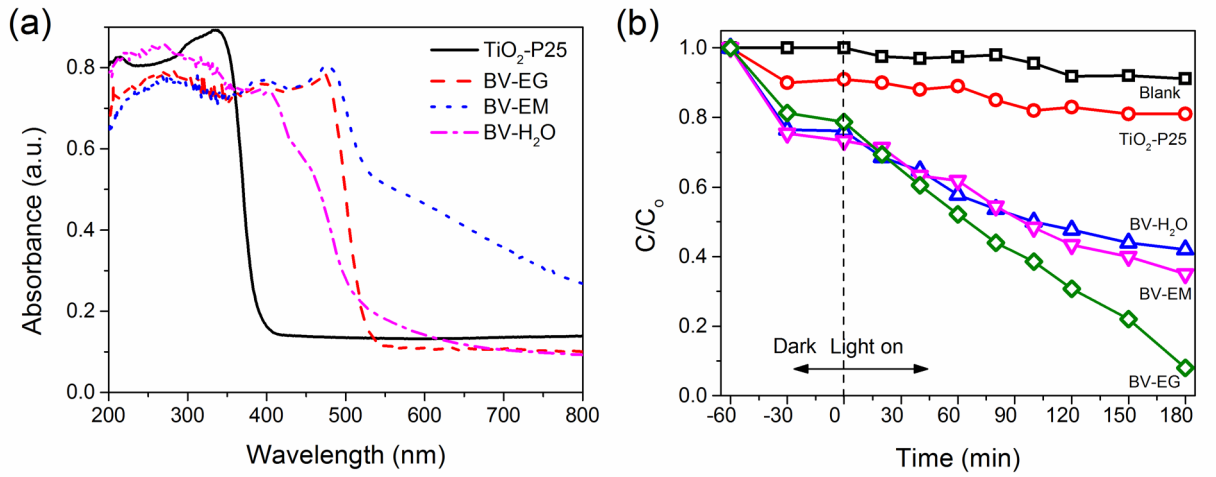

Fig. 3 UV-vis spectra of TiO_2-P25 and $BiVO_4$ samples (a), and photocatalytic decomposition of RhB as a function of irradiation time using TiO_2-P25, $BiVO_4$ samples and without catalyst (b).

Conclusion

Highly crystallized $BiVO_4$ powders with different morphology have been successfully synthesized using EG, EM, and H_2O act as a solvent. From XRD and SEM results, pure s-m $BiVO_4$ with oliver morphology was obtained in the present of EG, z-t $BiVO_4$ with rod morphology was obtained in the present of H_2O, and a mixture of s-m and z-t $BiVO_4$ with starflower morphology was obtained in the present of EM. Oliver-like $BiVO_4$ showed excellent catalytic activity for the decomposition of RhB under visible light as compared to that of starflower-like $BiVO_4$ and rod-like $BiVO_4$, and it is much higher than that of comercial TiO_2-P25 materials. The results indicate that the enhanced photocatalytic activity of $BiVO_4$ samples is most probably related to the morphology and structure phase of $BiVO_4$.

Acknowledgments

This research is funded by Ho Chi Minh City Department of Science and Technology, and Youth Development Scicence and Technology Center, Ho Chi Minh City Communist Youth Union, Vietnam.

References

[1] Y. Yang, R. Ouyang, L. Xu, N. Guo, W. Li, K. Feng, L. Ouyang, Z. Yang, S. Zhou, Y. Miao, Review: Bismuth complexes: synthesis and applications in biomedicine, J. Coord. Chem. 68 (2015) 379–397.

[2] Y. Z. Wang, W. Wang, H. Y. Mao, Y. H. Lu, J. G. Lu, J. Y. Huang, Z. Z. Ye, B. Lu, Electrostatic Self-Assembly of $BiVO_4$-Reduced Graphene Oxide Nanocomposites for Highly Efficient Visible Light Photocatalytic Activities, ACS Appl. Mater. Interfaces. 6 (2014) 12698–12706.

[3] L. Ye, Y. Su, X. Jin, H. Xie, C. Zhang, Recent advances in BiOX (X = Cl, Br and I) photocatalysts: synthesis, modification, facet effects and mechanisms, Environ. Sci. Nano. 1 (2014) 90.

[4] S. Tokunaga, H. Kato, a. Kudo, Selective preparation of monoclinic and tetragonal $BiVO_4$ with scheelite structure and their photocatalytic properties, Chem. Mater. 13 (2001) 4624–4628.

[5] B. I. Lee, R. K. Gupta, C. M. Whang, Effects of solvent and chelating agent on synthesis of solid oxide fuel cell perovskite, $La_{0.8}Sr_{0.2}CrO_{3-\delta}$, Mater. Res. Bull. 43 (2008) 207–221.

[6] J. Livage, M. Henry, C. Sanchez, Sol-gel chemistry of transition metal oxides, Prog. Solid State Chem. 18 (1988) 259–341.

[7] G. Li, Y. Ding, Y. Zhang, Z. Lu, H. Sun, R. Chen, Microwave synthesis of $BiPO_4$ nanostructures and their morphology-dependent photocatalytic performances, J. Colloid Interface Sci. 363 (2011) 497–503.

[8] X. Liang, S. Kuang, Y. Li, Solvothermal synthesis and luminescence of nearly monodisperse $LnVO_4$ nanoparticles, J. Mater. Res. 26 (2011) 1168–1173.

[9] A. Kudo, K. Ueda, H. Kato, I. Mikami, Photocatalytic O_2 evolution under visible light irradiation on $BiVO_4$ in aqueous $AgNO_3$ solution, Catal. Lett. 53 (1998) 229–230.

[10] X. Lin, L. Yu, L. Yan, H. Li, Y. Yan, C. Liu, H. Zhai, Visible light photocatalytic activity of $BiVO_4$ particles with different morphologies, Solid State Sci. 32 (2014) 61–66.

[11] C. Fu, G. Li, M. Zhao, L. Yang, J. Zheng, L. Li, Solvent-driven room-temperature synthesis of nanoparticles $BiPO_4$: Eu^{3+}., Inorg. Chem. 51 (2012) 5869–5880.

[12] Y. Zhao, Y. Xie, X. Zhu, S. Yan, S. Wang, Surfactant-free synthesis of hyperbranched monoclinic bismuth vanadate and its applications in photocatalysis, gas sensing, and lithium-ion batteries, Chemistry (Easton). 14 (2008) 1601–1606.

[13] G. Tan, L. Zhang, H. Ren, J. Huang, W. Yang, A. Xia, Microwave hydrothermal synthesis of N-doped $BiVO_4$ nanoplates with exposed (040) facets and enhanced visible-light photocatalytic properties, Ceram. Int. 40 (2014) 9541–9547.

[14] L. Chen, J. Wang, D. Meng, Y. Xing, C. Wang, F. Li, Y. Wang, X. Wu, Enhanced photocatalytic activity of hierarchically structured $BiVO_4$ oriented along {040} facets with different morphologies, Mater. Lett. 147 (2015) 1–3.

[15] L. Zhang, J. Long, W. Pan, S. Zhou, J. Zhu, Y. Zhao, X. Wang, G. Cao, Efficient removal of methylene blue over composite-phase $BiVO_4$ fabricated by hydrothermal control synthesis, Mater. Chem. Phys. 136 (2012) 897–902.

[16] Y. Sun, C. Wu, R. Long, Y. Cui, S. Zhang, Y. Xie, Synthetic loosely packed monoclinic $BiVO_4$ nanoellipsoids with novel multiresponses to visible light, trace gas and temperature. Chem. Commun. (Camb). (2009) 4542–4544.